Electronic Supplementary Material (ESI) for Journal of Materials Chemistry A.

Supplementary Information

Earth-abundant iron(III) species serves as a cocatalyst boosting the multi-electron reduction of IO_3^-/I^- redox shuttle in Z-scheme photocatalytic water splitting

Katsuya Murofushi,[a,†] Kanta Ogawa,[a,b,†] Hajime Suzuki,[a] Ryota Sakamoto,[a] Osamu Tomita,[a] Kosaku Kato,[c] Akira Yamakata,[c] Akinori Saeki,[d] Ryu Abe[a,b,*]

[a]Department of Energy and Hydrocarbon Chemistry, Graduate School of Engineering, Kyoto University, Nishikyo-ku, Kyoto 615-8510, Japan.

[b]AIST-Kyoto University Chemical Energy Materials Open Innovation Laboratory (ChEM-OIL), National Institute of Advanced Industrial Science and Technology (AIST), Sakyo-ku, Kyoto 606-8501, Japan.

[c]Graduate School of Engineering, Toyota Technological Institute, 2-12-1 Hisakata, Tempaku, Nagoya 468-8511, Japan

[d]Department of Applied Chemistry, Graduate School of Engineering, Osaka University, 2-1 Yamadaoka, Suita, Osaka 565-0871, Japan

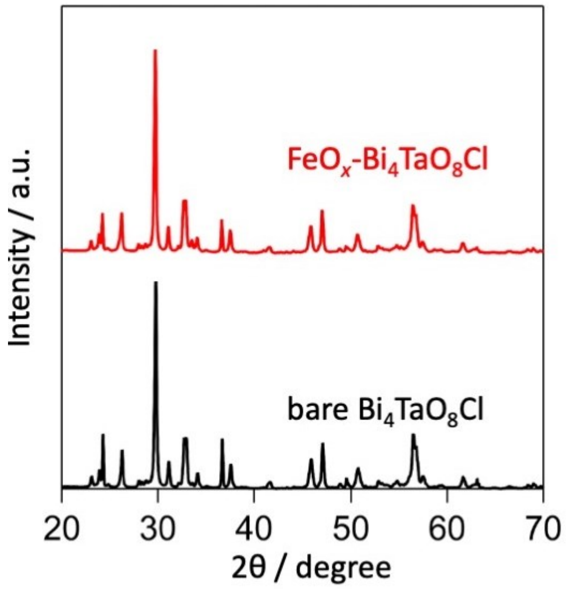

Fig. S1 XRD pattern of bare and FeO_x-Bi_4TaO_8Cl samples.

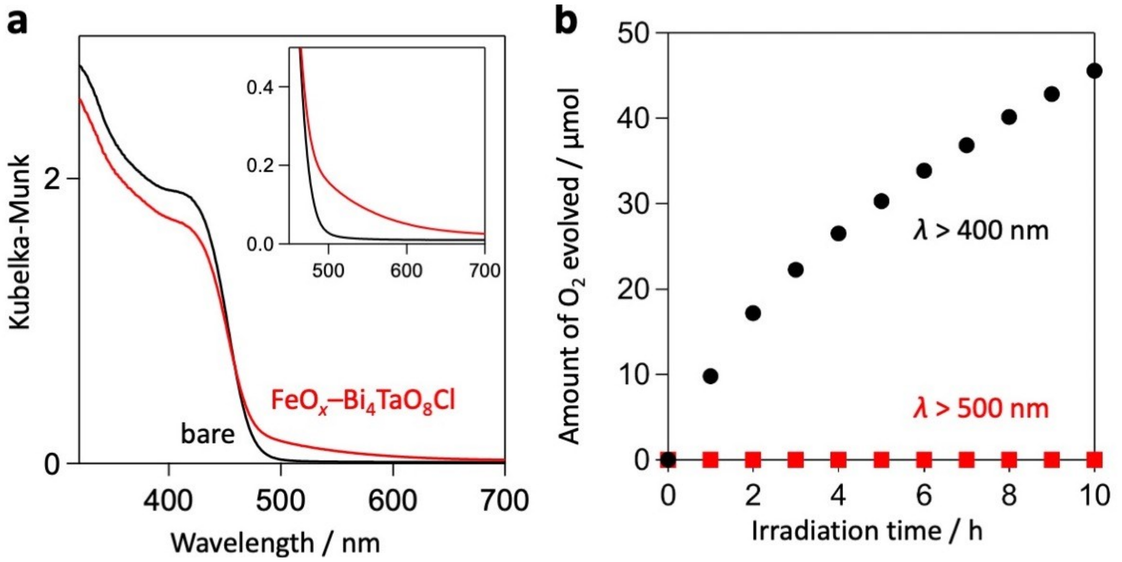

Fig. S2 a, DRS of bare and FeO_x- Bi_4TaO_8Cl. b, Time courses of O_2 evolution over FeO_x-Bi_4TaO_8Cl in aqueous $NaIO_3$ solution (4 mM) under visible-light (λ > 400 or > 500 nm) irradiation. FeO_x-Bi_4TaO_8Cl shows an absorption shoulder at 480-620 nm. However, upon excitation with 500 nm, negligible O_2 evolution was observed. We then assign the absorption shoulder to light scattering by the FeO_x particles, rather than the direct interfacial charge transfer.

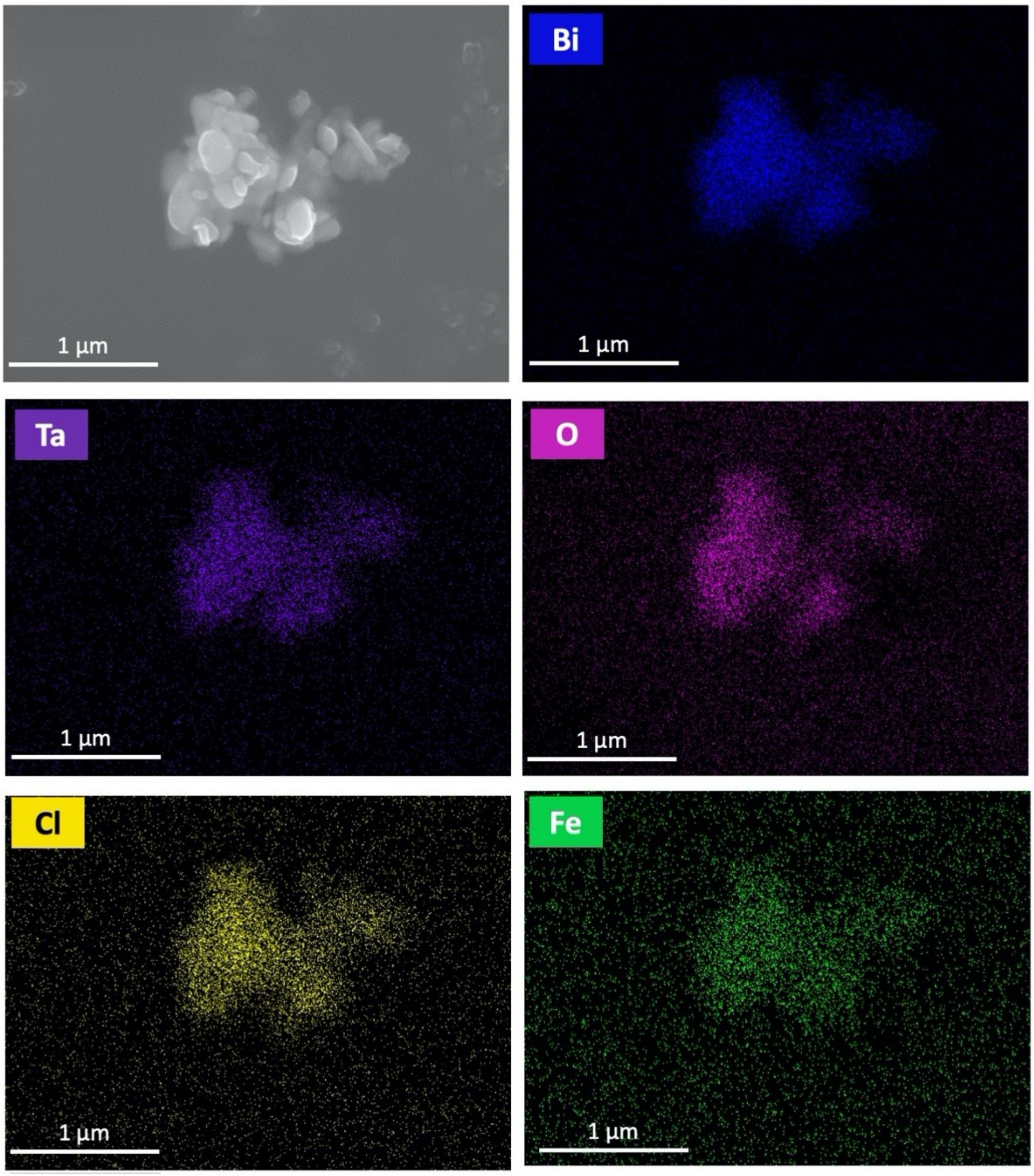

Fig. S3 SEM image and SEM-EDS elemental mapping of FeO_x-Bi_4TaO_8Cl.

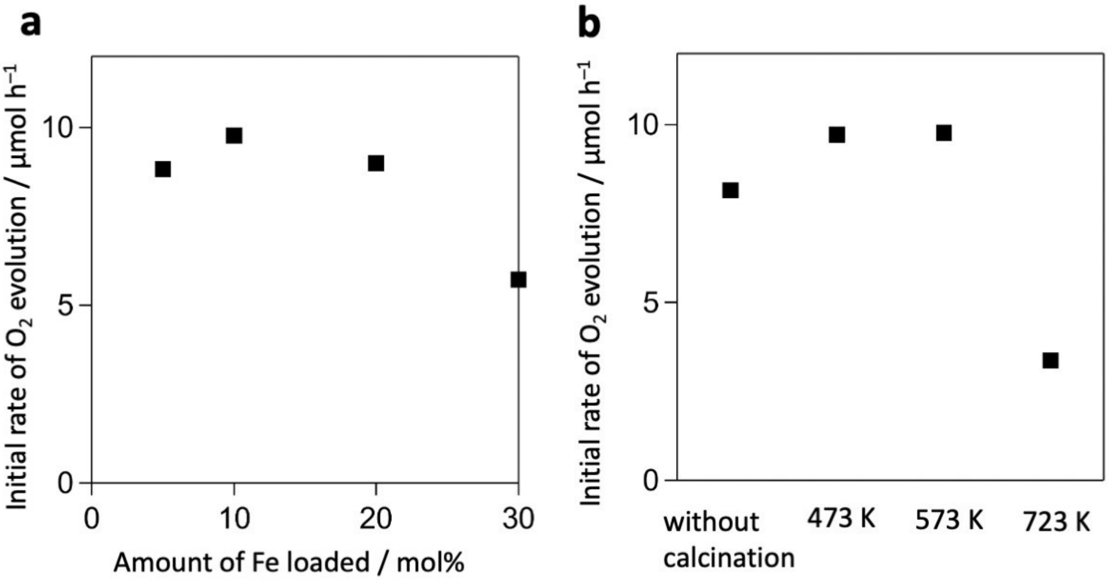

Fig. S4 The effect of the loading amount (a) and the calcination temperature (b) for FeO_x-loading on photocatalytic activity.

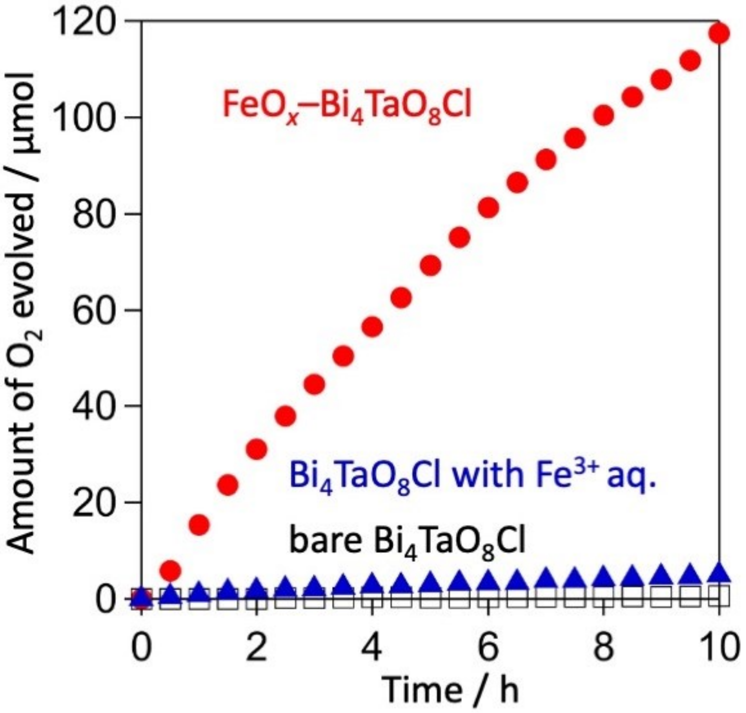

Fig. S5 The effect of the adding of the Fe^{3+} cation of same amount as the loaded FeO_x (17 µmol) into the reaction solution ($NaIO_3$ solution (4 mM), pH = 2.5) on O_2 evolution under visible-light (λ > 400 nm) irradiation. Mere adding of Fe^{3+} to the reaction solution (blue triangle) show much lower O_2 evolution activity than the FeO_x-Bi_4TaO_8Cl. The small amount of O_2 on bare Bi_4TaO_8Cl sample by the addition of Fe^{3+} was probably generated through the reduction of Fe^{3+} to Fe^{2+} by photoexcited electrons.

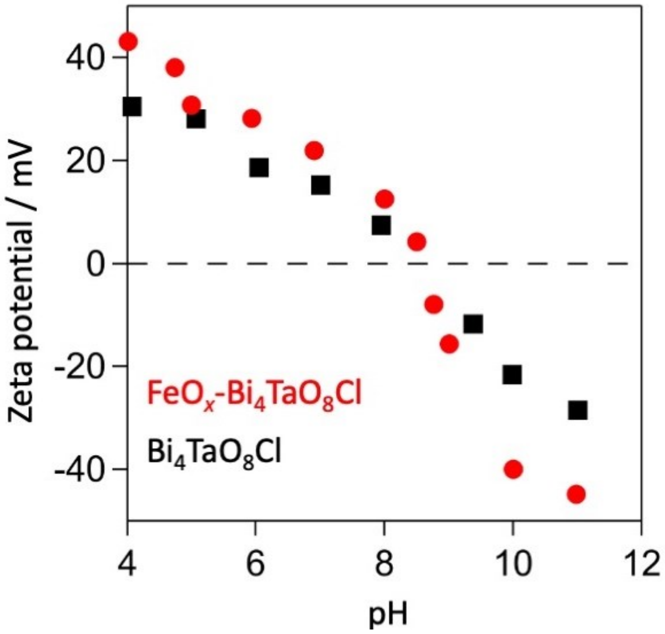

Fig. S6 The pH dependence of Zeta potentials of bare and FeO_x-Bi_4TaO_8Cl.

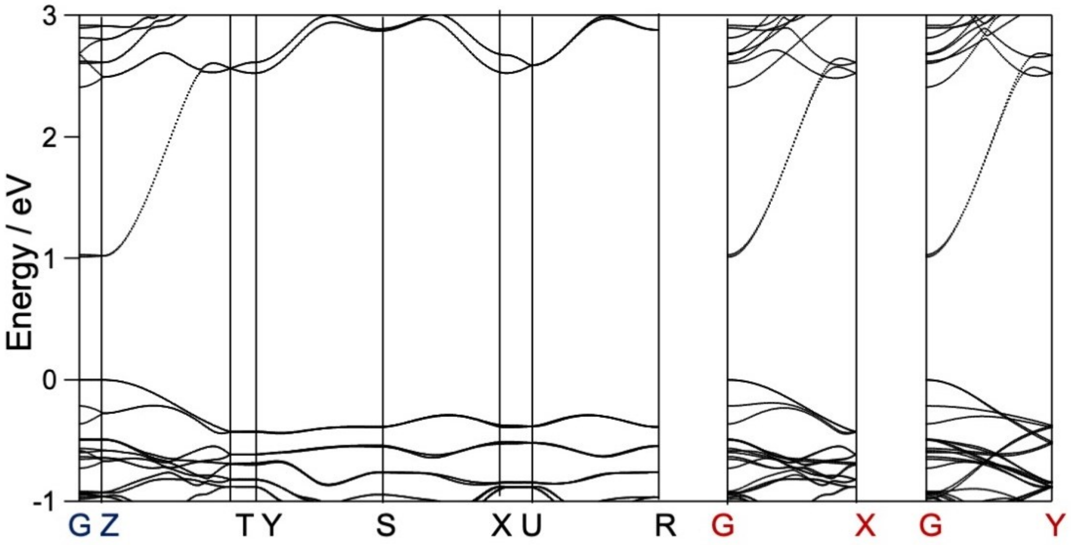

Fig. S7 Band structure of Bi_4TaO_8Cl. Effective masses were estimated from the DFT results. The mean of the relative effective masses in the in-plane (Γ-X and Γ-Y) directions are 0.25 m_0 and 1.4 m_0 for electrons and holes, respectively.

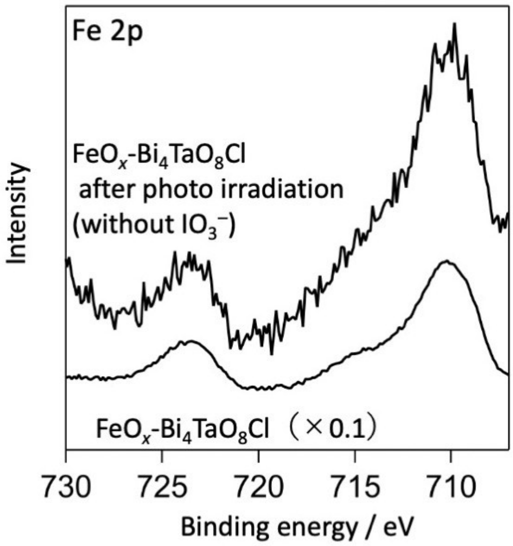

Fig. S8 XP spectra focusing on Fe 2p region for FeO_x-Bi_4TaO_8Cl before and after photoirradiation (10 h) in the absence of IO_3^-. The FeO_x species should underwent facile oxidation by the ambient O_2.

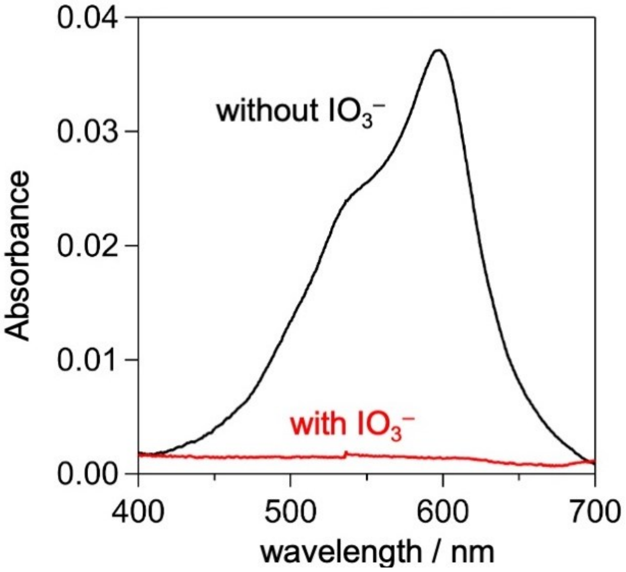

Fig. S9 Absorption spectra of Fe^{2+} produced in the reaction solution after the photo-irradiation on FeO_x-Bi_4TaO_8Cl with or without IO_3^- in the reaction solution.

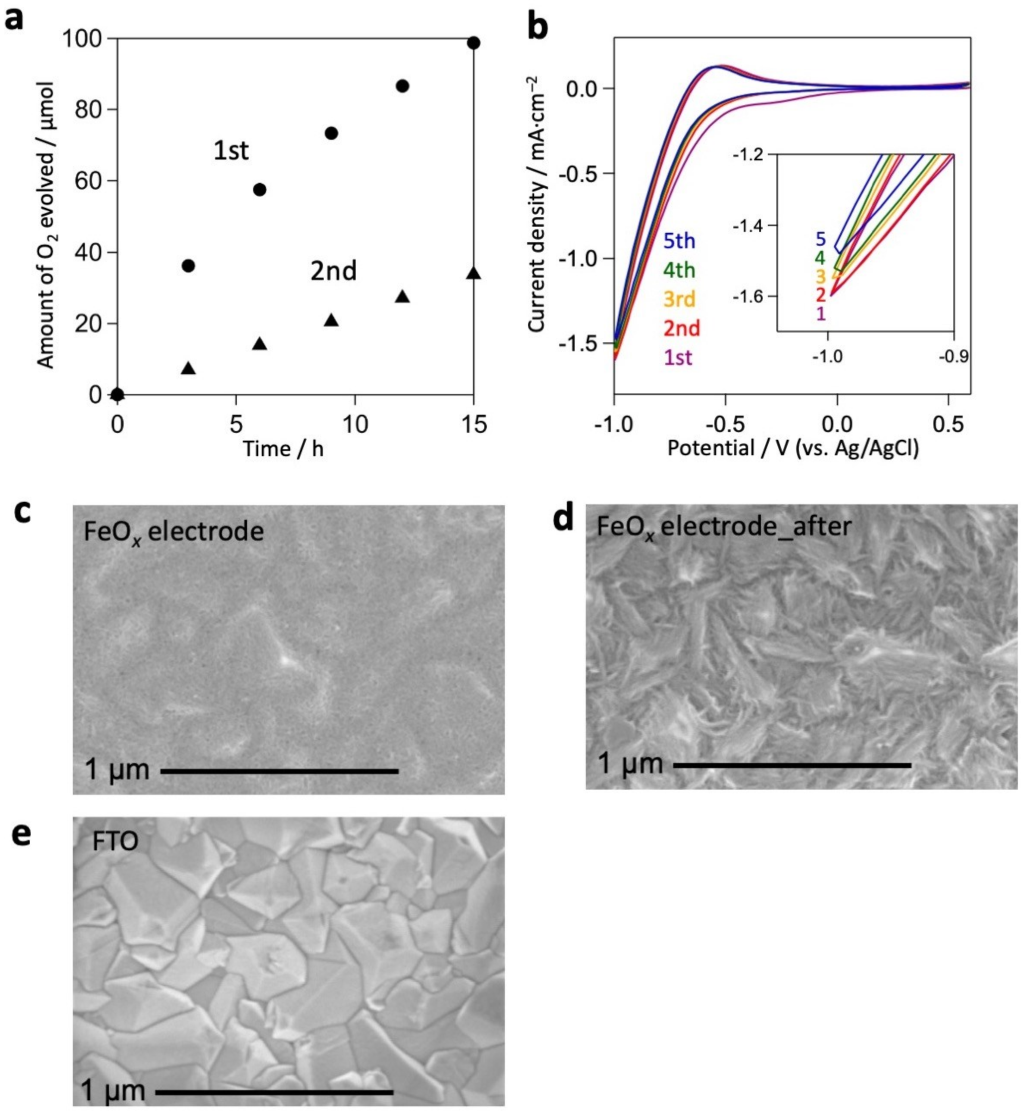

Fig. S10 a, Repeatability test for the photocatalytic O_2 evolution over FeO_x-Bi_4TaO_8Cl in $NaIO_3$ aqueous solution (4 mM) under visible light irradiation (λ > 400 nm). b, Cyclic voltammogram for a FeO_x/FTO working electrode in 0.1 M Na_2SO_4 solution containing 4 mM $NaIO_3$. c,d, SEM images of the FeO_x/FTO working electrode before and after the electrochemical operation. e, SEM image of bare FTO. In the cyclic voltammetry, the catalytic current for the reduction of IO_3^- decreased by repeating the cycle. The morphology of FeO_x/FTO changed after the electrochemical operation, where the aggregation of FeO_x proceeded in SEM.

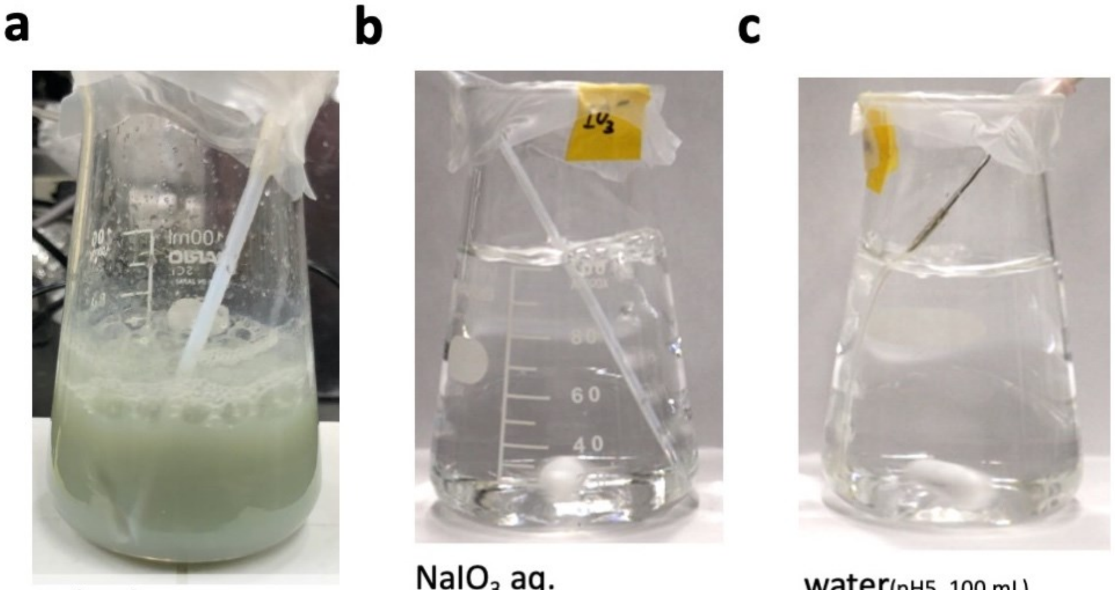

$Fe(OH)_2$

$NaIO_3$ aq.
(4 mM, pH5, 100 mL)

water(pH5, 100 mL)

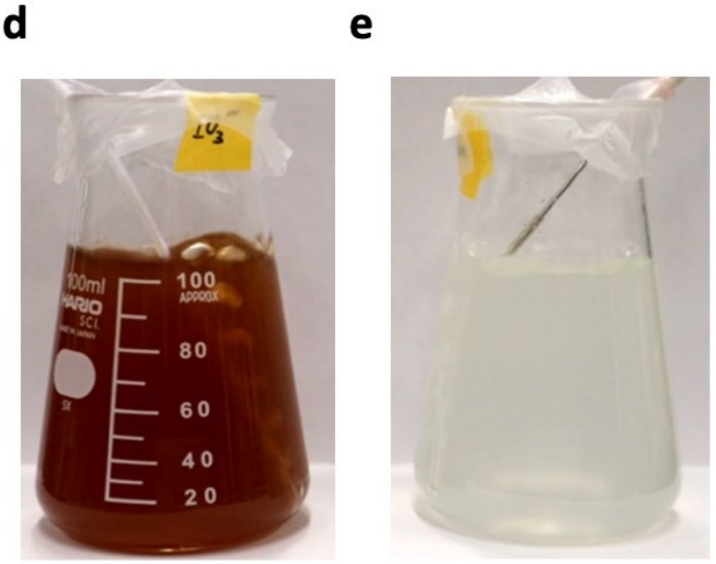

$Fe(OH)_2+IO_3^-$

$Fe(OH)_2$ + water

Fig. S11 Pictures of as-prepared $Fe(OH)_2$ colloidal solution (a), $NaIO_3$ aqueous solution (b), water (c). $Fe(OH)_2$ colloidal solution (0.4 mmol as Fe) after adding to IO_3^- aqueous solution (4 mM, 100 mL) (d) and water (e).

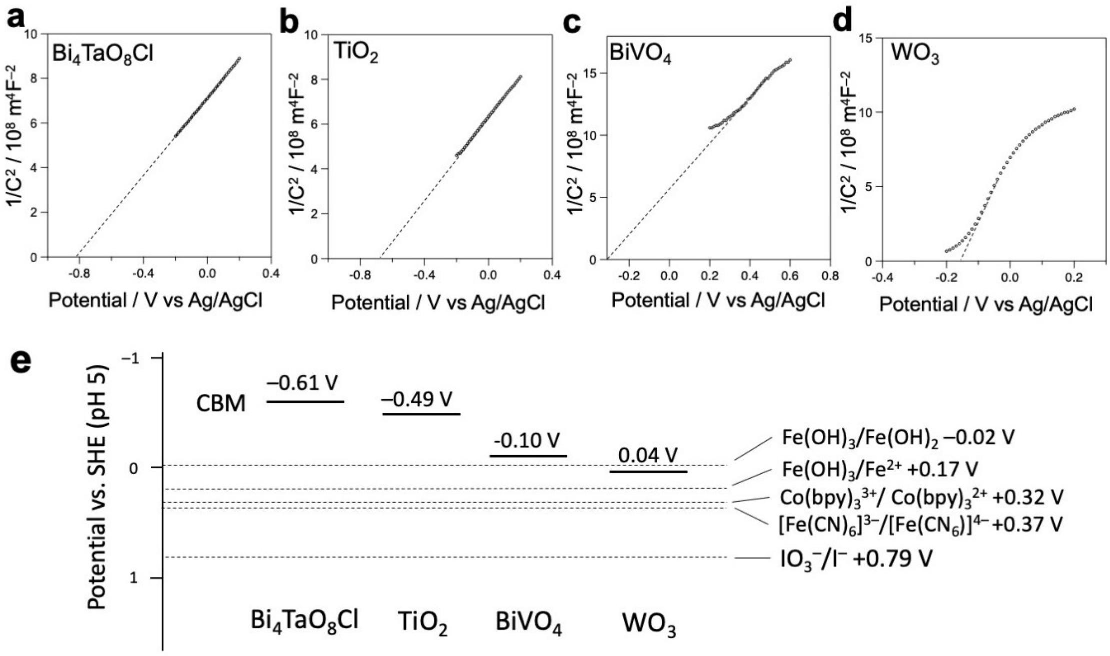

Fig. S12 a-d, Mott–Schottky plots for Bi_4TaO_8Cl (a), TiO_2 (b), $BiVO_4$ (c), WO_3 (d) in 0.5 M Na_2SO_4 solution (pH = 5). e, CBM positions of these samples estimated from the Mott-Schottky plots along with redox potentials of Fe^{III}/Fe^{II}, IO_3^-/I^-, $Co(bpy)_3^{3+}$/ $Co(bpy)_3^{2+}$, $[Fe(CN)_6]^{3-}/[Fe(CN_6)]^{4-}$.